JSIAM Letters Vol.10 (2018) pp.33–36 ©2018 Japan Society for Industrial and Applied Mathematics

Mathematical modeling and analysis of ErbB3 and EGFR dimerization process for the gefitinib resistance

Keiko Itano[1], Takeshi Ito[2], Shuji Kawasaki[3], Yoshinori Murakami[2] and Takashi Suzuki[1]

[1] Graduate School of Engineering Science, Osaka University, 1-3 Machikaneyama-cho, Toyonaka-shi, Osaka 560-8531, Japan
[2] Division of Molecular Pathology, The Institute of Medical Science, The University of Tokyo, 4-6-1 Shirokanedai, Minato-ku, Tokyo 108-8639, Japan
[3] Graduate School of Engineering, Iwate University, 4-3-5 Ueda, Morioka-shi, Iwate 020-8551, Japan

E-mail *itano@sigmath.es.osaka-u.ac.jp*

Received August 25, 2017, Accepted March 14, 2018

Abstract

Lung cancer is the leading cause of cancer death. Dimerization and phosphorylation of the receptor tyrosine kinase are involved in the malignant progression of cancers and drug resistance. Focusing on the EGFR-ErbB3 dimerization, we build a mathematical model using ordinary differential equations (ODEs). By classifying the molecules into two groups, we sum molecular ODEs into two groups and solve them explicitly. From these solutions, all molecule concentrations and their equilibria can be derived theoretically. Based on the theoretical solutions, we determine the dimerization behavior and a key parameter. Our model can be applied to similar dimerization networks.

Keywords dimerization, grouping, EGFR, ErbB3, gefitinib resistance

Research Activity Group Mathematical Medicine

1. Introduction

Lung cancer is the leading cause of cancer death worldwide, and lung adenocarcinoma is the most common subtype of lung cancer. In East Asia, mutation of the *epidermal growth factor receptor* (*EGFR*) gene is the most frequent cause of lung adenocarcinoma. Gefitinib, one of the EGFR tyrosine kinase inhibitors (EGFR-TKI), is clinically used as a molecularly targeted drug for lung adenocarcinoma in individuals harboring *EGFR* mutations. The effect of gefitinib is dramatic; however, tumor resistance to the drug inevitably arises in a few years. The known mechanisms of gefitinib resistance are the T790M secondary mutation of the *EGFR* gene ($\sim 50\%$) and amplification of the *MET* gene, which encodes a receptor tyrosine kinase ($4 \sim 20\%$). The T790M mutation is believed to sterically block the binding of gefitinib, while MET activates the downstream signaling of EGFR through ErbB3, which is another receptor of tyrosine kinase. The restoration of the phosphorylated EGFR-ErbB3 heterodimer is considered to be the cause of gefitinib resistance. Fig. 1 is an image of the gefitinib resistance mechanism with *MET* amplification.

As a first step to understand this resistance mechanism, we focus on the EGFR-ErbB3 dimerization process. Several mathematical models have been built for this kind of dimerization process [1–3], which show the time courses of the molecules by simulation. However, these mathematical models cannot be solved explicitly because they are nonlinear.

Previously we built ordinary differential equation (ODE) models for the extended Matrix metalloproteinase2 (MMP2) activation network and derived ODE solutions and equilibria theoretically by classifying molecules to certain groups and summing molecular ODEs to group ODEs [4–6]. For the EGFR-ErbB3 dimerization, we built ODEs of the EGFR-ErbB3 dimerization and solved these ODEs by classifying the molecules into a monomer group and a dimer group. In the case of EGFR-ErbB3 dimerization, the molecules are classified into monomer and dimer groups. The molecular concentrations and the equilibria are also derived explicitly by this method.

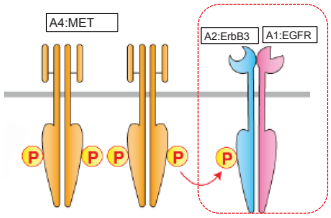

Fig. 1. Gefitinib resistance mechanism with MET amplification.

2. Mathematical model of dimerization

We focus on the dimerization process of EGFR and ErbB3, because EGFR-ErbB3, as a heterodimer, causes gefitinib resistance by MET according to the work by Engelmann et al. [7]. We built ODEs in order to understand the effect of the reaction rules on the behavior of the pathway network. By understanding the effects of chemical reaction rules and their order on the behav-

ior of the network, the evolution of the network can be predicted from the formations of complexes in it. The complex formations correspond to the chemical reaction rules and orders. As a simplification, let A_1 be EGFR (harboring mutation), A_2 be ErbB3, A_3 be gefitinib, and A_4 be MET. Dimerization and phosphorylation of receptor tyrosine kinases are involved in the malignant progression of cancers. A_1 and A_2 can form both homodimers (A_1A_1 and A_2A_2) and heterodimers (A_1A_2). Phosphorylated A_1A_1 and A_1A_2 dimers generate proliferation signals, while the phosphorylated A_2A_2 dimer does not, as A_2 does not have kinase activity. A_3 inhibits the phosphorylation of A_1A_1. A_4 forms only homodimers (A_4A_4), which phosphorylate the dimers including A_2 (A_1A_2 and A_2A_2). The restoration of phosphorylated A_1A_2 is considered to be the cause of gefitinib resistance.

Firstly, we consider a signaling network which contains A_1 and A_2. A_1 and A_2 form three kinds of dimers: A_1A_1, A_1A_2, and A_2A_2. The chemical reactions for these phases can be expressed as follows:

The dimerization of A_1 and A_2 is given by

$A_1 + A_1 \leftrightarrow A_1A_1,$
$A_1 + A_2 \leftrightarrow A_1A_2,$
$A_2 + A_2 \leftrightarrow A_2A_2.$

The concentrations of molecules A_1, A_2, A_1A_1, A_1A_2, and A_2A_2 at time t are denoted by $X_1(t)$, $X_2(t)$, $X_3(t)$, $X_4(t)$ and $X_5(t)$. The evolution equations of the concentrations are derived from the law of mass action and from the law of mass conservation. Firstly, let us consider a network consisting of A_1 and A_2 monomers. A scheme of molecular reactions is shown in Fig. 2. To obtain the law of mass action in the signaling network, we define k_1, k_2, and k_3 as association rate constants between A_1 and A_1, A_2 and A_2, and A_1 and A_2 in the absence of their ligands. The dissociation rate constants of A_1A_1, A_2A_2, and A_1A_2 are defined by l_1, l_2, and l_3.

From the law of mass action the following equations can be obtained for the pathway network:

$$\begin{aligned}
\frac{dX_1}{dt} &= -k_1X_1^2 + 2l_1X_3 - k_3X_1X_2 + l_3X_4,\\
\frac{dX_2}{dt} &= -k_2X_2^2 + 2l_2X_5 - k_3X_1X_2 + l_3X_4,\\
\frac{dX_3}{dt} &= \frac{k_1}{2}X_1^2 - l_1X_3,\\
\frac{dX_4}{dt} &= k_3X_1X_2 - l_3X_4,\\
\frac{dX_5}{dt} &= \frac{k_2}{2}X_2^2 - l_2X_5.
\end{aligned} \tag{1}$$

By assuming that this network is closed, the total number of A_1 or A_2 is preserved. From the law of mass conservation the following equations can be derived for A_1 or A_2:

$$\begin{aligned}
X_1(t) + 2X_3(t) + X_4(t) &= X_1(0),\\
X_2(t) + 2X_5(t) + X_4(t) &= X_2(0).
\end{aligned} \tag{2}$$

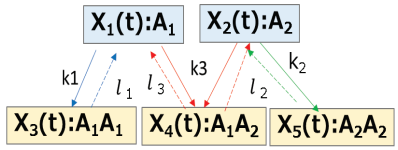

Fig. 2. Dimerization diagram of the first reaction phase.

3. Grouping and the group ODE model

We separate molecules into two groups: monomers (ξ) and dimers (η). The group concentrations at time t are defined as follows:

$$\begin{aligned}
\xi(t) &= X_1(t) + X_2(t),\\
\eta(t) &= X_3(t) + X_4(t) + X_5(t).
\end{aligned} \tag{3}$$

According to (2) and (3), the law of mass conservation for the groups can be written as

$$\xi(t) + 2\eta(t) = X_1(0) + X_2(0). \tag{4}$$

The values of association and dissociation rate constants and initial molecular concentrations are required for the calculation. Firstly, we assume that association rates $k = k_1 \approx k_2 \approx k_3$ and dissociation rates $l = l_1 \approx l_2 \approx l_3$. By summing the molecular ODEs in (1), by using (2)–(4) two group ODEs can be obtained:

$$\begin{aligned}
\frac{d\xi(t)}{dt} &= -k\xi(t)^2 - l\xi(t) + l\xi(0),\\
\frac{d\eta(t)}{dt} &= -\frac{1}{2}\frac{d\xi(t)}{dt}.
\end{aligned} \tag{5}$$

The equilibrium of the monomer group ξ concentration $\xi^*_\pm$ can be obtained from (5) as follows:

$$\xi^*_\pm = \frac{-l \pm \sqrt{l^2 + 4kl\xi(0)}}{2k}. \tag{6}$$

The group ξ concentration at time t is

$$\xi(t) = \frac{\xi^*_+ - C\xi^*_- e^{-\beta t}}{1 - Ce^{-\beta t}}, \tag{7}$$

where

$$\beta = k(\xi^*_+ - \xi^*_-) = \sqrt{l^2 + 4kl\xi(0)} > 0,$$

$$C = \frac{X_1(0) + X_2(0) - \xi^*_+}{X_1(0) + X_2(0) - \xi^*_-}.$$

From (4), the dimer group concentration $\eta(t)$ and its equilibrium η^* can be derived:

$$\eta(t) = \frac{\xi(0) - \xi(t)}{2}, \tag{8}$$

$$\eta^* = \frac{\xi(0) - \xi^*}{2}. \tag{9}$$

The group concentrations and their equilibria are obtained from the association and dissociation constants and from the initial monomer concentrations.

Next, we rebuild the model based on real data using Refs. [8–10]. From these data, the values of l_1/k_1, l_2/k_2, and l_1 are $2.31 \times 10^{-11}[D]$, $5.82 \times 10^{-13}[D]$, and

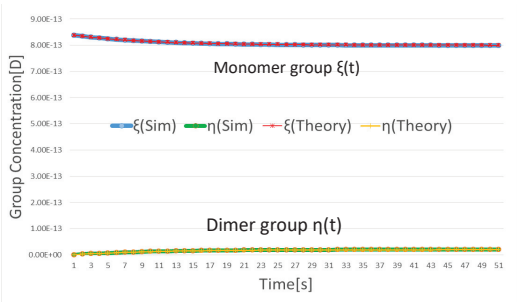

Fig. 3. Time evolution of monomer group concentration $\xi(t)$ and dimer group concentration $\eta(t)$ from the simulation by ODE and theoretical solutions.

$0.724[/s]$, respectively. It should be noted that in this study the unit D indicates mol/dm^2, as these molecular reactions take place on the cell membrane. From these values, k_1 and k_2 are calculated as $6.0\times10^{10}[/Ds]$ and $1.7\times10^{12}[/Ds]$, respectively, with the assumption $l_2 = 1[/s]$. By applying dimensional analysis to (1), we identify k_3 as $1.5\times10^{11}[/Ds]$ by assuming $l_3 = 1[/s]$. The numbers of A_1 and A_2 on one cell surface are experimentally determined as $10^5 \sim 10^6$ and $10^3 \sim 10^4$, respectively, using cancer cell lines [11,12]. Then, the molecular concentrations on one cell membrane are determined as $8.3\times10^{-13} \sim 8.3\times10^{-12}[D]$ and $8.3\times10^{-15} \sim 8.3\times10^{-14}[D]$, respectively, if we assume that the average cell surface area is $2000[\mu m^2]$. The initial concentration of the molecules are expected to be $X_1(0) = 8.3\times10^{-13}[D]$ and $X_2(0) = 8.3\times10^{-15}[D]$. The initial concentrations of the dimers are $X_3(0) = X_4(0) = X_5(0) = 0[D]$, with no dimers are expected at the beginning. We define $k_r = 3.0\times10^{10}[/Ds]$ and $l_r = 1.0[/s]$. The association rate constants are approximated as $k_1 \approx 2k_r$, $k_2 \approx 60k_r$, $k_3 \approx 5k_r$, and $l_1 = l_2 = l_3 = l_r$.

In this case, the two group ODEs can be written as follows:

$$\begin{aligned}\frac{d\xi(t)}{dt} &= -2k_r(\xi(t)^2 + 3X_1(t)X_2(t) + 29X_2(t)^2) + 2l_r\eta(t)\\ \frac{d\eta(t)}{dt} &= k_r(\xi(t)^2 + 3X_1(t)X_2(t) + 29X_2(t)^2) - l_r\eta(t)\end{aligned} \tag{10}$$

Compared to (5), the group ODEs in (10) have extra terms, $k_rX_1(t)X_2(t)$ and $k_rX_2(t)^2$ in the right-hand side. The orders of $k_r\xi(t)^2$, $k_rX_1(t)X_2(t)$, and $k_rX_2(t)^2$ are $\mathcal{O}(10^{-13})$, $\mathcal{O}(10^{-15})$, and $\mathcal{O}(10^{-17})$, respectively. Thus, $k_rX_2(t)^2$ is negligible compared to $k_r\xi(t)^2$. Although $k_rX_1(t)X_2(t)$ is small it is definitely not negligible. To understand the effect of the terms on the pathway network, we simulate (10) and (5) with association and dissociation rates k_r and l_r.

Fig. 3 shows the time evolution of the group concentrations obtained from the simulation by (10) and the theoretical solution of (5) given by (7) and (8). If $3k_rX_1(t)X_2(t)$ and $29k_rX_2(t)^2$ in (10) are negligible, then (10) is equal to (5). The difference between (5) and (10) simulation results is two decimal places, which is due to the term $k_rX_1(t)X_2(t)$. The results indicate that the group ODEs in (5) decide the network behavior mainly.

4. Molecule concentration and equilibrium

In the previous section, the monomer and dimer group concentrations were derived from the group ODEs in (5), which are the main equations for the network. We assume that the association rate $k = k_1 \approx k_2 \approx k_3$. The substitution of group concentrations $\xi(t)$ and $\eta(t)$ into (1) gives

$$\begin{aligned}\frac{dX_1(t)}{dt} &= -(k\xi(t) + l)X_1(t) + lX_1(0),\\ \frac{dX_2(t)}{dt} &= -(k\xi(t) + l)X_2(t) + lX_2(0),\\ \frac{dX_3(t)}{dt} &= -lX_3(t) + \frac{1}{2}kX_1(t)^2,\\ \frac{dX_4(t)}{dt} &= -lX_4(t) + kX_1(t)X_2(t),\\ \frac{dX_5(t)}{dt} &= -lX_5(t) + \frac{1}{2}kX_2(t)^2.\end{aligned} \tag{11}$$

The molecular equations above correspond to the generalized equation, $dX(t)/dt = -A(t)X(t) + f(t)$. The solution of the generalized equation is given by

$$X(t) = e^{-\int_0^t A(s)ds}\left(\int_0^t e^{-\int_0^s A(u)du} f(s)ds + \text{const}\right). \tag{12}$$

Its equilibrium X^* can be written as

$$X^* = \frac{f^*}{A^*}. \tag{13}$$

The equilibrium solutions of the monomer concentrations are

$$\begin{aligned}X_1^* &= \frac{X_1(0)l_1}{k\xi^* + l_1} = \frac{X_1(0)}{X_1(0) + X_2(0)}\xi^*,\\ X_2^* &= \frac{X_2(0)l_1}{k\xi^* + l_1} = \frac{\xi^*}{X_1(0) + X_2(0)}X_2(0).\end{aligned} \tag{14}$$

Nevertheless, the equilibrium of the dimer concentrations can also be obtained as

$$\begin{aligned}X_3^* &= \frac{k}{2l}X_1^{*2} = \frac{k}{2l}\left(\frac{X_1(0)}{X_1(0) + X_2(0)}\right)^2\xi^{*2},\\ X_4^* &= \frac{k}{l}X_1^*X_2^* = \frac{k}{2l}\frac{2X_1(0)X_2(0)}{(X_1(0) + X_2(0))^2}\xi^{*2},\\ X_5^* &= \frac{k}{2l}X_2^{*2} = \frac{k}{2l}\left(\frac{X_2(0)}{X_1(0) + X_2(0)}\right)^2\xi^{*2}.\end{aligned} \tag{15}$$

Fig. 4 shows the concentrations of all molecules from simulation and theory, while Fig. 5 shows an enlarged version of the figure from it. The equilibrium values of all molecules are shown in Table 1. The theoretical results are in good agreement with the simulation results.

5. Conclusion

We build an ODE model of biochemical reactions in the EGFR-ErbB3 dimerization process, which is an important process in the gefitinib resistance mechanism. Classifying the molecules into monomer and dimer groups, the solutions and equilibria of the groups and

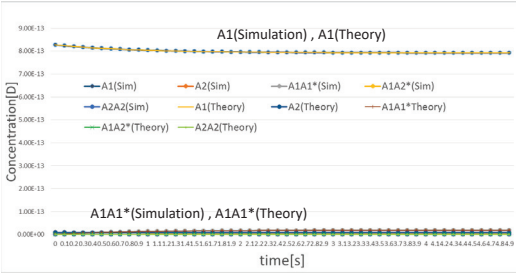

Fig. 4. Time evolution of concentration of monomers and dimers, obtained from ODE simulation and theoretical solutions. The ODE simulation results and the theoretical results are in good agreement. The monomer A_1 concentration is much higher than those of the other molecules.

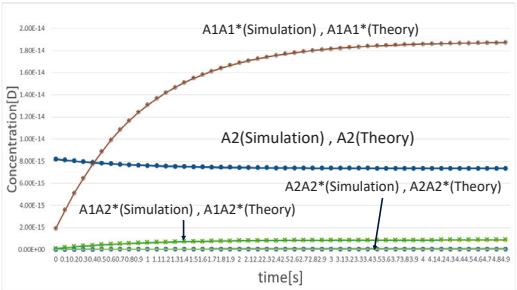

Fig. 5. Enlarged figure of Fig. 4 showing the time evolution of monomers and dimers except for A_1. They are obtained from ODE simulation and theoretical solutions.

Table 1. Equilibrium concentrations of molecules calculated by simulation and theory.

	Simulation Result	**Theoretical Result**
$X_1 : A_1$	$7.92 \times 10^{-13}[D]$	$7.92 \times 10^{-13}[D]$
$X_2 : A_2$	$7.34 \times 10^{-15}[D]$	$7.34 \times 10^{-15}[D]$
$X_3 : A_1A_1^*$	$1.87 \times 10^{-14}[D]$	$1.87 \times 10^{-14}[D]$
$X_4 : A_1A_2^*$	$8.69 \times 10^{-16}[D]$	$8.69 \times 10^{-16}[D]$
$X_5 : A_2A_2$	$4.57 \times 10^{-17}[D]$	$4.57 \times 10^{-17}[D]$

molecular ODEs are derived theoretically, using only association and dissociation rate parameters and initial monomer concentrations. We find that the group concentration ODEs (5) govern the pathway network behavior mainly. Using (11) and (15), we theoretically predict the molecule concentrations and equilibria and the convergence time to their equilibria, without ODE simulation. Then, an obvious relationship between the molecules in the network can be obtained. The initial concentration $X_1(0) + X_2(0)$ of the monomer group is a key parameter in this network.

Our results can be applied to similar kinds of dimerization networks, with similar chemical reaction rules. If the dimerization network is heterogenous, it is possible to apply this model by using compartments, in which the molecules are homogenous.

Acknowledgments

This work is supported by JSPS KAKENHI, Grant Numbers JP16K45678, JP16H06576, JP26247013, JP17H05993, and the Core-to-Core Program, Mathematical Oncology International Research Network.

References

[1] H. Shankaran, H. S. Wiley and H. Resat, Modeling the Effects of HER/ErbB1-3 Coexpression on Receptor Dimerization and Biological Response, Biophys. J., **90** (2006), 3993–4009.

[2] M. A. Lemmon, Ligand-induced ErbB receptor dimerization, Exp. Cell Res., **315** (2009), 638–648.

[3] M. M. Pryor, M. P. Steinkamp, A. M. Halasz, Y. Chen, S. Yang, M. S. Smith, G. Zahoransky-Kohalmi, M. Swift, X. Xu, D. Hanien, N, Volkmann, D. S. Lidke, J. S. Edwards and B. S. Wilson, Orchestration of ErbB3 Signaling through Heterointeractions and Homointeractions, eds. Jennifer Lippincott-Schwartz, Mol. Biol. Cell, **26.22** (2015), 4109–4123.

[4] T. Saitou, K. Itano, D. Hoshino, N. Koshikawa, M. Seiki, K. Ichikawa and T. Suzuki, Control and inhibition analysis of complex formation processes, Theor. Biol. Med. Model., **9** (2012), 33.

[5] S. Kawasaki, D. Minerva, K. Itano and T. Suzuki, Finding Solvable Units of Variables in Nonlinear ODEs of ECM Degradation Pathway Network, Comput. Math. Methods Med., **2017** (2017), 1–15.

[6] K. Itano and T. Suzuki, Mathematical Modelling and Analysis of the Enhanced ECM Degradation Pathway Network with N Monomers (in Japanese), Trans. JSIAM, **26** (2016), 44–83.

[7] J. A. Engelman, K. Zejnullahu, T. Mitsudomi, Y. Song, C. Hyland, J. O. Park, N. Lindeman, C. M. Gale, X. Zhao, J. Christensen, T. Kosaka, A.J. Holmes, A. M. Rogers, F. Cappuzzo, T. Mok, C. Lee, B. E. Johnson, L. C. Cantley and P. A. Janne, MET amplification leads to gefitinib resistance in lung cancer by activating ERBB3 signaling, Science, **316** (2007), 1039–1043.

[8] Y. Teramura, J. Ichinose, H. Takagi, K. Nishida, T. Yanagida and Y. Sako, Single-molecule analysis of epidermal growth factor binding on the surface of living cells, EMBO J., **25** (2006), 4215–4222.

[9] M. Hiroshima, Y. Saeki, M. Okada-Hatakeyama, and Y. Sako, Dynamically varying interactions between heregulin and ErbB proteins detected by single-molecule analysis in living cells, Proc. Natl. Acad. Sci. USA, **109** (2012), 13984–13989.

[10] S. T. Low-Nam, K. A. Lidke, P. J. Cutler, R. C. Roovers, P. M. P. van Bergen en Henegouwen, B. S. Wilson and D. S. Lidke, ErbB1 dimerization is promoted by domain co-confinement and stabilized by ligand-binding, Nat. Struct. Mol. Biol., **18** (2011), 1244–1249.

[11] Z. Novy, P. Barta, J. Mandikova, M. Laznicek and F. Trejtnar, A comparison of in vitro methods for determining the membrane receptor expression in cell lines, Nucl. Med. Biol., **39** (2012), 893–896.

[12] C. Panke, D. Weininger, A. Haas, F. Schelter, T. Schlothauer, S. Bader, R. Sircar, H. P. Josel, U. Baer, H. Burtscher, O. Mundigl, M. Grote, U. Brinkmann and C. Sustmann, Quantification of cell surface proteins with bispecific antibodies, Protein Eng. Des. Sel., **26** (2013), 645–654.